CHAPTER 7

RESULTS AND DISCUSSION

The first part of the results addresses the analysis and reactions of the lixiviant, which is the iron(III).

7.1 E_h and pH determination

A sample of 98% zinc sulphide from Riedel de Haën was used as a synthetic sphalerite sample and leached in the experimental set-up as described above. Samples were withdrawn from the reaction mixture and pH and E_h valued determined. The samples were then returned to the reaction mixture.

7.2 Calculation of E_h values

The Eh values were calculated according to the following equation:

$$E_h = E^0 - \frac{RT}{F}\ln(\frac{[\mathrm{Re}\,d]}{[Ox]}) \qquad (65)$$

where

E^0 is the standard reversible potential of the electrode couple

R is the universal gas constant (8.324 $J \cdot K^{-1} \cdot mol^{-1}$)

T is the absolute temperature in Kelvin

F is the Faraday constant (96 500 C $mole^{-1}$).

The notation [Red] represents the concentration of the iron species that appear on the reduced side of the electrode reaction and the

notation [Ox] represents the concentration of the iron species that appear on the oxidised side of the electrode reaction.

The results obtained during the leaching tests showing the relationship between Fe(III) concentration and the measured and calculated E_h during the leaching of the synthetic sphalerite are presented in table 10. The ΔE_h values (calculated from experimental determinations minus measured values) correspond well with the difference of 199 mV between the standard hydrogen electrode (SHE) and Ag/AgCl electrode, as was reported by Corrosion Doctors (1999).

Table 10: Relationship between Fe(III) concentration and the measured and calculated Eh during the leaching of the synthetic sphalerite

Initial $[Fe^{3+}]$ = 0.1mol/dm^3				
Time	Fe^{3+}	Calculated	Measured	Delta Eh
(s)	mol/dm^3	E_h (mV)	E_h (mV)	E_h (mV)
30	0.100	911	734	177
900	0.053	775	584	191
1800	0.055	777	579	198
3600	0.056	778	581	197
Initial $[Fe^{3+}]$ = 0.2mol/dm^3				
Time	Fe^{3+}	Calculated	Measured	Delta Eh
(s)	mol/dm^3	E_h (mV)	E_h (mV)	E_h (mV)
30	0.200	932	728	204
900	0.163	812	633	179
1800	0.153	809	633	176
3600	0.156	810	628	182

Initial $[Fe^{3+}]$ = 0.3mol/dm^3				
Time	Fe^{3+}	Calculated	Measured	Delta Eh
(s)	mol/dm^3	E_h (mV)	E_h (mV)	E_h (mV)
30	0.300	945	734	211
900	0.266	826	623	203
1800	0.250	824	614	210
3600	0.256	825	625	200

From table 11 it is clear that for all concentrations of $FeCl_3$, the available Fe(III) concentration is about 100% after 30 seconds. After 900 seconds the iron(II) starts to increase, while the iron(III) diminishes.

Table 11: Summary of iron (III) and iron (II) concentrations during the leach test of the synthetic sphalerite

	Initial $[Fe^{3+}]$= 0.3mol/dm^3						
Time	Fe^{3+}			Fe^{2+}			Total
(s)	mg/l	mol/dm^3	%	mg/l	mol/dm^3	%	[Fe]
30	16744	0.30	99.9	56	0.00	0.3	0.30
900	14882	0.27	88.8	2418	0.04	14.4	0.31
1800	13971	0.25	83.4	2429	0.04	14.5	0.29
3600	14282	0.26	85.2	2418	0.04	14.4	0.30
	Initial $[Fe^{3+}]$=0.2mol/dm^3						
30	11158	0.20	99.9	56	0.00	0.5	0.20
900	9109	0.16	81.6	2403	0.04	21.5	0.21
1800	8524	0.15	76.3	2450	0.04	21.9	0.20
3600	8696	0.16	77.9	2445	0.04	21.9	0.20
	Initial $[Fe^{3+}]$=0.1mol/dm^3						
30	5574	0.10	99.8	56	0.00	1.0	0.10
900	2933	0.05	52.5	2597	0.05	46.5	0.10
1800	3075	0.06	55.1	2535	0.05	45.4	0.10
3600	3106	0.06	55.6	2474	0.04	44.3	0.10

It is clear from this that after 2000 seconds the reaction with synthetic sphalerite was completed, after which the Fe^{3+} concentration remained constant. It is also clear that for the 0.3 mol/dm^3 reaction mixture, a reasonable excess of Fe^{3+} was still available (about 0.25

mol/dm^3). For the 0.1 mol/dm^3, only half of the original Fe^{3+} (about 0.06 mol/dm^3) was left.

Figure 16 represents the reaction of the Fe^{3+} exhaustion during the oxidation of the sphalerite.

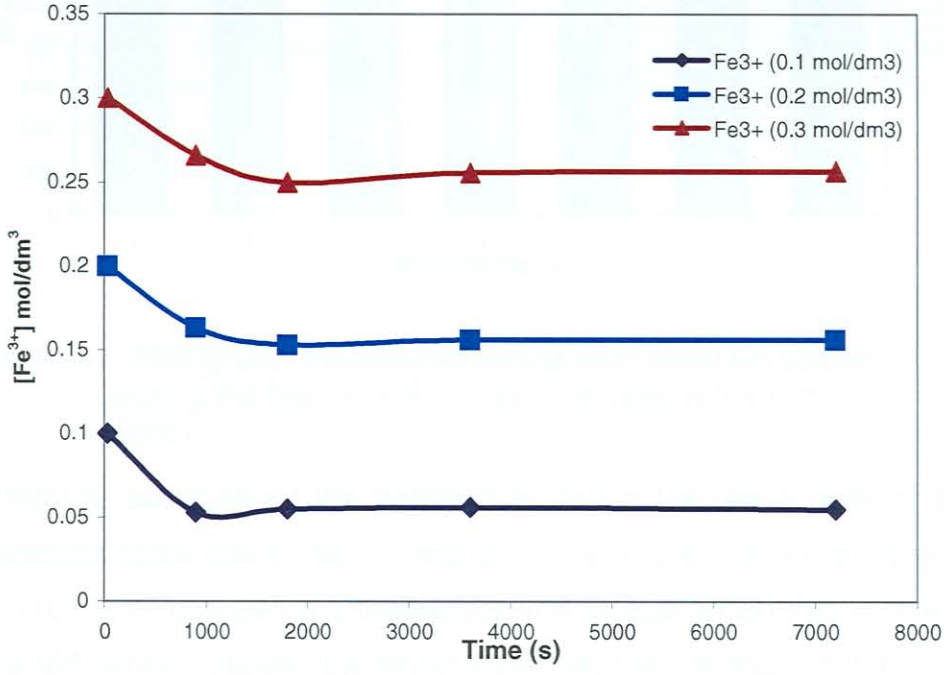

Figure 16: Plot of [Fe^{3+}] in mol/dm3 showing the depletion during the leaching of synthetic sphalerite in $FeCl_3$ medium

7.3 Leach tests

Figure 17 is a graphical representation of one of the leach tests where calculated Eh values are compared with the measured values. From this figure can be seen that there is a good correlation between the calculated and measured values.

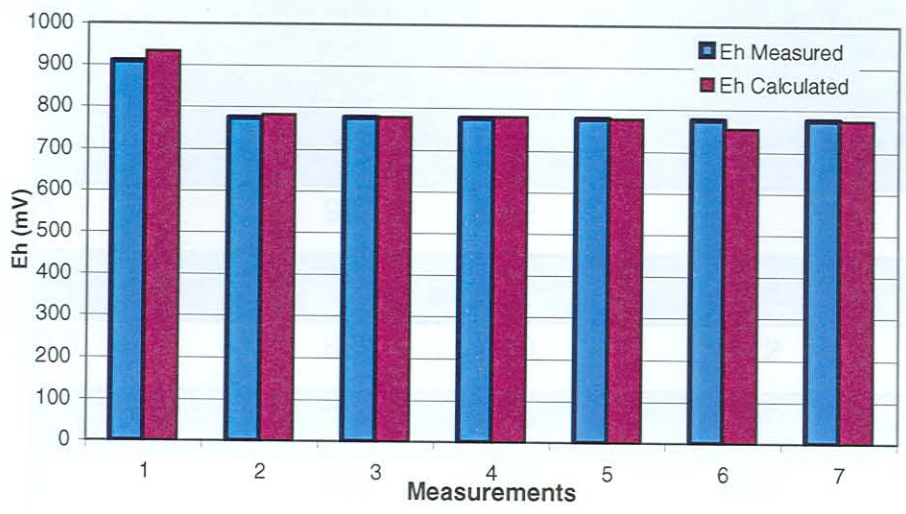

Figure 17: Histogram of measured versus calculated Eh values during the leaching of synthetic sphalerite (corrected to SHE)

Table 12 summarises the parameters during the leach tests of the synthetic sphalerite in the 0.2 mol/dm^3 test. There was a discrepancy of -193.9mV between the theoretical and measured Eh that is due to the difference between the silver/silver chloride electrode potential of 199 mV in a saturated potassium chloride solution and the standard hydrogen electrode (SHE). It can be noted that the temperature was controlled between 76.7°C and 84.3°C. The pH was measured between 0.7 and 1.89. The values recorded after two hours, however, seem erratic, which could be due to the length of the experiment and measurement at a higher temperature.

Table 12: Eh (corrected to SHE), pH and temperature values during the leach test			
Time (h)	Eh (mV)	pH	Temperature (°C)
0	927	1.02	79
0.25	832	1.05	83.4
0.5	832	1.09	80.2
1	827	1.05	76.7
2	813	1.89	80.4
4	812	1.34	84.3
6	624	0.7	79.6

7.4 Results and discussion of the zinc part of the reaction

Figure 18 shows the effect of the same initial sphalerite concentration of 12.7% Zn and different lixiviant (leach solution) concentrations. It seems that the reaction does not depend much on the lixiviant concentration. The effect will be discussed during the kinetic evaluation. Zn concentration was determined as described in 6.4.1.

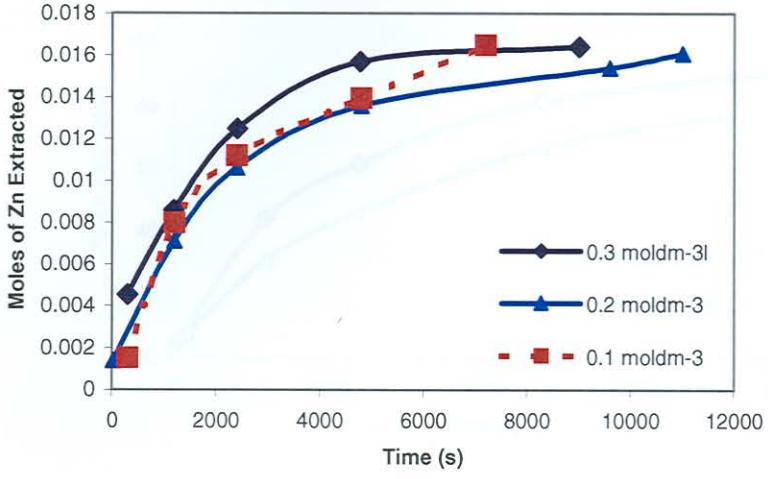

Figure 18: Graph moles of Zn extracted at the same initial sphalerite concentration of 12.7% Zn, with different $FeCl_3$ concentrations at 90°C.

Figure 19 represents the reproducibility of the method. Identical conditions were applied two weeks apart. The reproducibility and repeatability are very good.

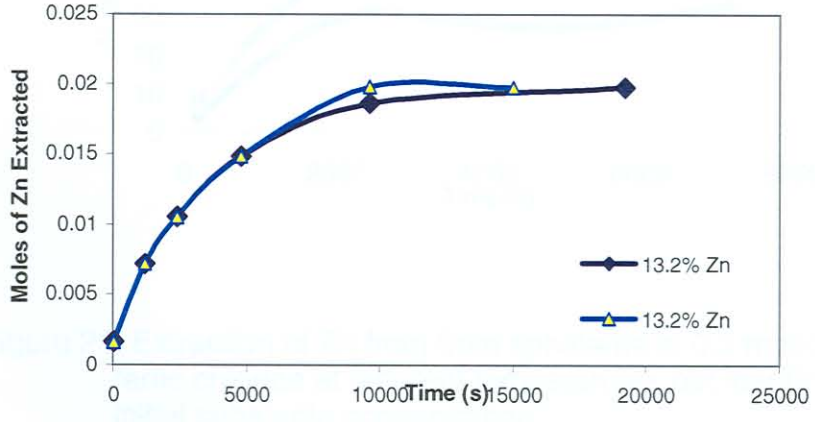

Figure 19: Graph moles of zinc extracted at the same initial sphalerite concentration, $FeCl_3$ concentration and temperature (0.2 mol/dm^3 ferric chloride at 80°C)

Figure 20 shows the effect of different initial sphalerite concentrations with the same lixiviant concentration at the same temperature.

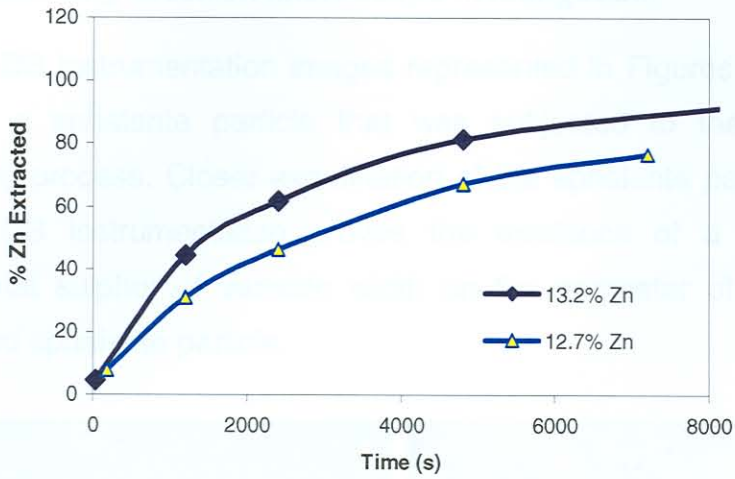

Figure 20: Graph indicating the % of zinc extracted at different initial sphalerite concentrations in 0.3 mol/dm^3 ferric chloride at 80°C

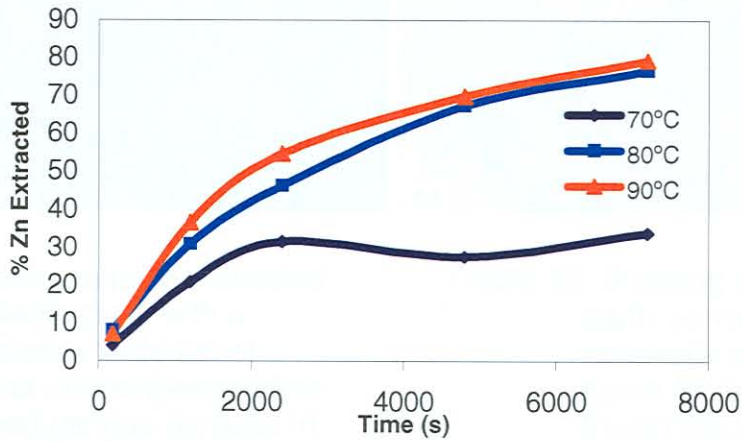

Figure 21: Extraction of Zn from from sphalerite in 0.3 mol/dm^3 ferric chloride at different temperatures but identical initial sphalerite concentration.

From figure 21 it is clear that the kinetics at 70°C are too slow for proper extraction of the zinc from the sphalerite. The best extraction that could be achieved was in the region of 30%, while the extractions at 80˚C and 90˚C were closer to 80% at the same time interval.

7.5 Scanning Electron Microscope Investigation

SEM-EDS instrumentation images represented in Figures 22 and 23 shows a sphalerite particle that was subjected to the Fe^{2+}/Fe^{3+} leaching process. Closer examination of the sphalerite particle using SEM-EDS instrumentation proves the existence of a coating of elemental sulphur of variable width on the perimeter of this partly digested sphalerite particle.

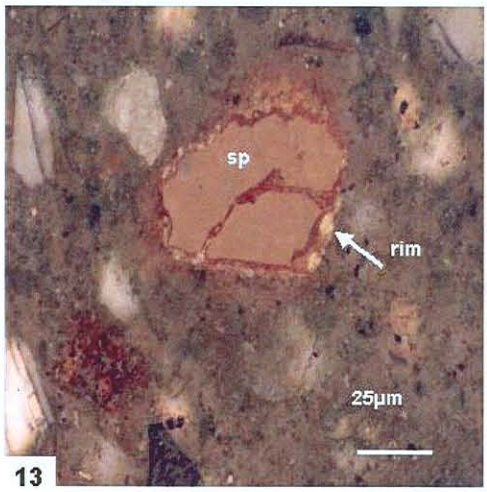

Figure 22: Showing a partly corroded sphalerite grain with a moderately wide rim of sulphur and embedded fine-grained gangue particles in reflected light, partly crossed nicols

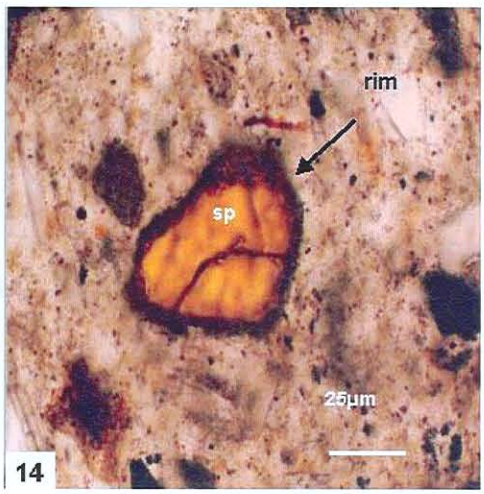

Figure 23: Showing the same partly corroded sphalerite grain as in figure 22 in transmitted plane light

sp = sphalerite

This phenomenon may be explained by the mixed control model which will be discussed in section 7.7.4. An attempt was made to make predictions about the rate-controlling step on the basis of leaching data.

7.6 Barium extraction

During the test work it was noticed that initially barium started leaching very well, with the barium ions in solution increasing. This

phenomenon was reversed by the resultant decrease in barium ions after about 20 minutes. The effect can be seen in figure 24. The conclusion was drawn that a complex reaction was taking place and that barium was competing for one of the sulphur species in solution, thereby assimilating one of the reaction products that could have an effect the rate of the reaction. Barium comcentrations were determined as described in 6.4.1.

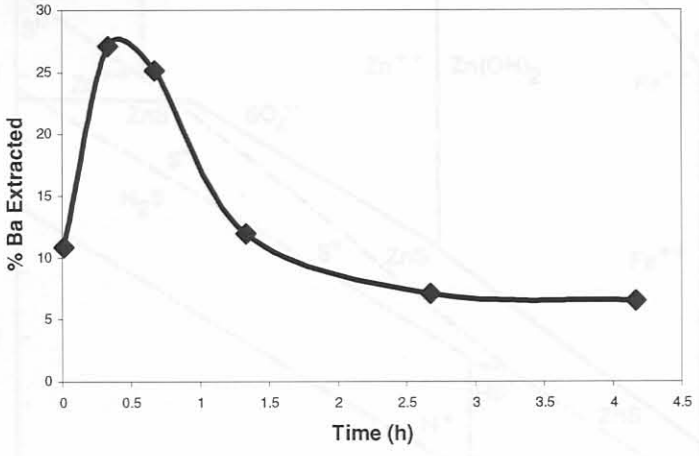

Figure 24: Extraction of barium from sphalerite in ferric chloride medium showing the extraction curve. Leaching conditions: 80°C and 0.2 mol/dm3 $FeCl_3$

If the Pourbaix diagram in figure 25 is considered, it seems possible for sulphur to exist as an SO_4^{2-} species in the region above pH 2 and at an E_h lower than 790 mV. This could lead to the formation of $BaSO_4$

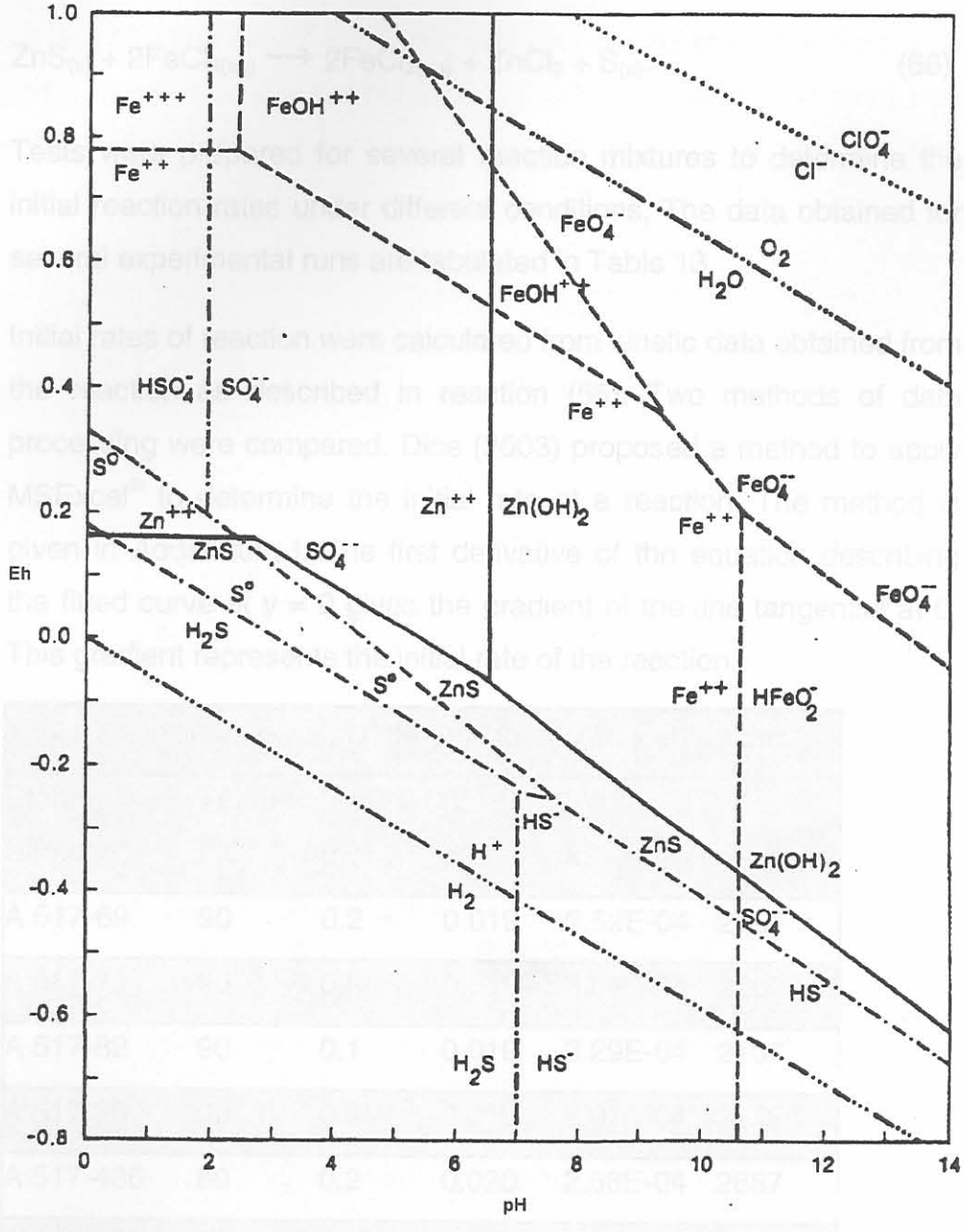

Figure 25: Pourbaix diagram for sphalerite in aqueous solution at 25°C (Bobeck and Su (1985))

7.7 Kinetic tests

7.7.1 The method of initial rates

The following reaction was considered to be the reaction between sphalerite and Ferric chloride:

$$ZnS_{(s)} + 2FeCl_{3(aq)} \longrightarrow 2FeCl_{2(aq)} + ZnCl_2 + S_{(s)}. \quad (66)$$

Tests were prepared for several reaction mixtures to determine the initial reaction rates under different conditions. The data obtained for several experimental runs are tabulated in Table 13.

Initial rates of reaction were calculated from kinetic data obtained from the reaction as described in reaction (65). Two methods of data processing were compared. Dice (2003) proposed a method to apply MSExcel® to determine the initial rate of a reaction. The method is given in Addendum I. The first derivative of the equation describing the fitted curve at y = 0 gives the gradient of the line tangential at 0. This gradient represents the initial rate of the reaction.

Table 13: Initial rates with different starting concentrations

Starting Sample	Temp (^{O}C)	[$FeCl_3$] mol	[ZnS] mol	k	$t_{1/2}$ (s)
A 517-69	90	0.2	0.019	2.52E-04	2751
A 517-75	90	0.2	0.019	3.04E-04	2280
A 517-82	90	0.1	0.019	3.29E-04	2107
A 517-88	90	0.3	0.019	3.07E-04	2258
A 517-486	80	0.2	0.020	2.58E-04	2687
A 517-100	70	0.2	0.019	1.51E-04	4590
A 517-493	80	0.2	0.020	3.10E-04	2236
A 517-63	90	0.2	0.019	3.65E-04	1899
A 517-656	80	0.3	0.012	6.26E-04	1107
A 517-664	80	0.3	0.012	8.00E-04	866

A plot of x (fraction of appearing species) versus extraction time (zero order kinetics) did not produce a straight line, as can be seen from figure 26. Evidently, this reaction does not support zero order kinetics.

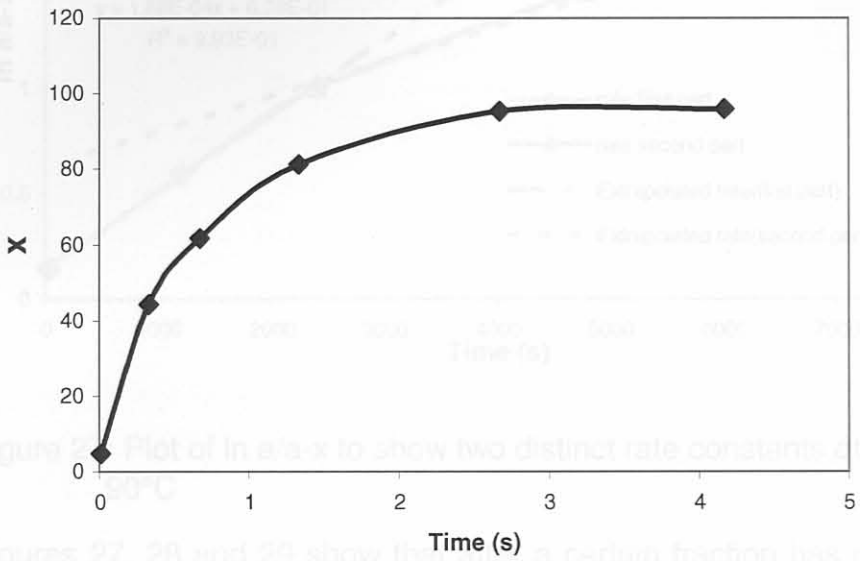

Figure 26: Plot of x against time, where x represents the fraction of Zn^{2+} forming. Leaching conditions: 80°C, 0.2 mol/dm3 $FeCl_3$ and 13.2% sphalerite

A plot of ln A or ln a_0/a_0-x as explained in section 5.4, on the other hand, rendered two distinct straight lines for each plot.

In an attempt to determine the activation energy, first-order plots (figures 27, 28 and 29) were constructed. The most obvious order was somewhere between zero and first order.

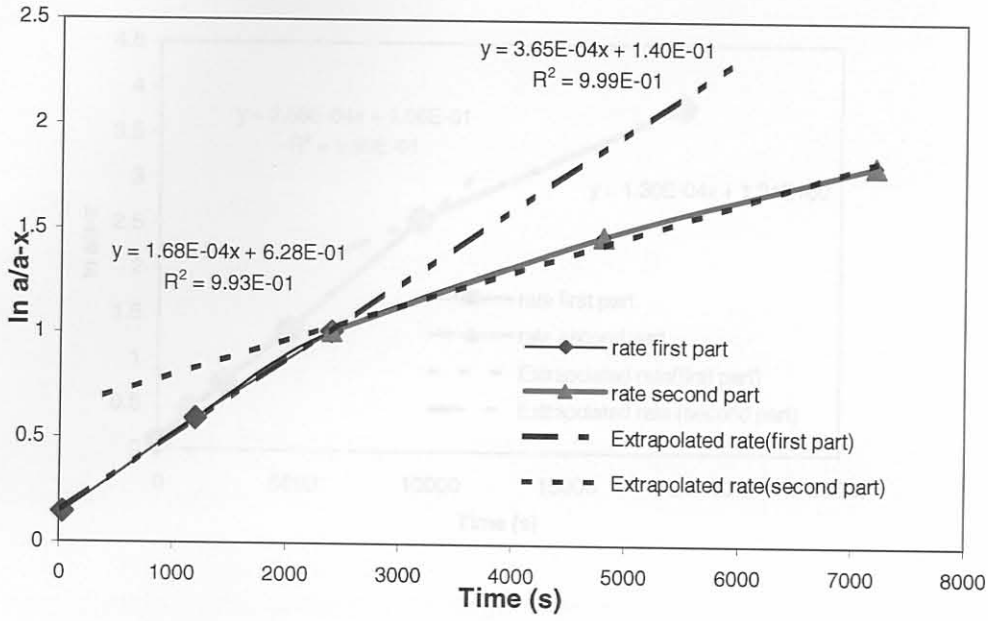

Figure 27: Plot of ln a/a-x to show two distinct rate constants at 90°C

Figures 27, 28 and 29 show that after a certain fraction has reacted, the rate constant changes. This can only be possible if this is not a true first-order reaction, or that the reaction mechanism changes after a certain amount of product has been formed. It would also be a complex reaction, consisting of a number of reaction steps, with different reaction steps being the rate – determining steps at different stages of the overall reaction.

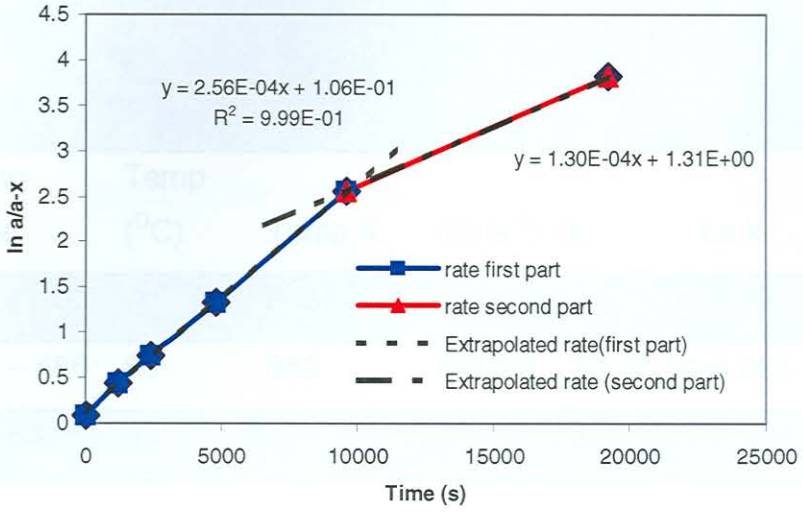

Figure 28: Plot of ln a/a-x at 80°C to show two distinct rate constants

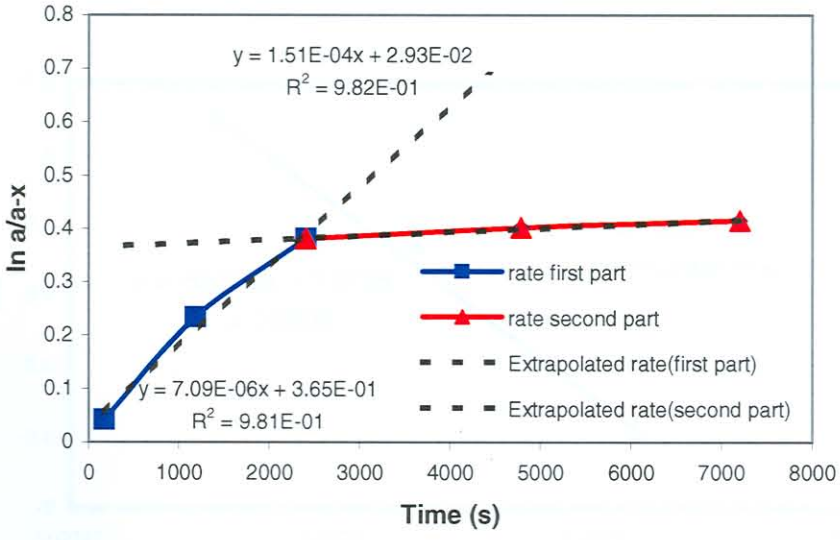

Figure 29: Plot of ln a/a-x at 70°C to show two distinct rate constants

Values obtained from the plot of ln a_0/a_0-x versus time are represented in table 14.

Table 14: Calculations for the Arrhenius plot for the first part of the reaction.

Starting sample	Temp (^{O}C)	Temp K	1/t (s^{-1})	k	Ln k
A 517 – 100	70	343	0.0029	1.51E-04	-8.798
A 517 – 486	80	353	0.0028	2.57E-04	-8.266
A517_63	90	363	0.0028	3.65E-04	-7.916

The activation energy was determined for the first part of the reaction by using the gradients of that part of the reaction. The plot for determining E_a is shown in figure 30.

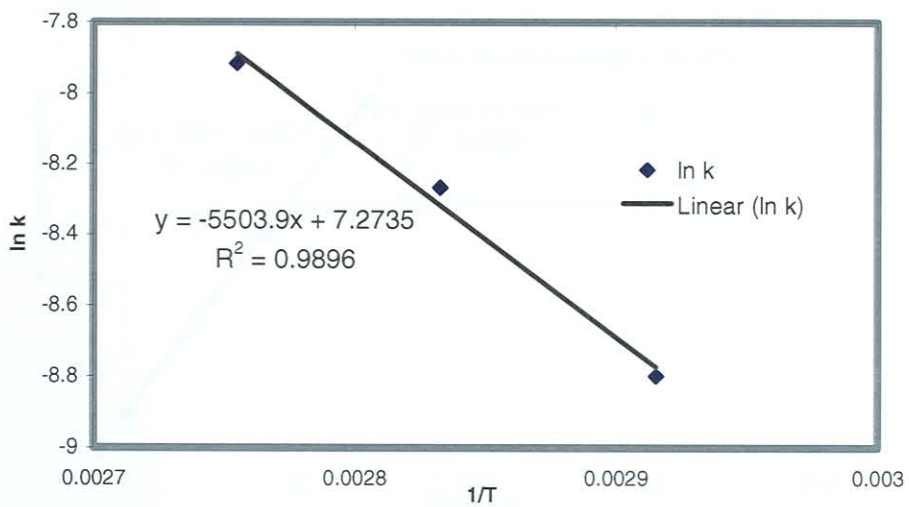

Figure 30: Arrhenius plot to show the relationship between the rate constant k and temperature in K for determining E_a for initial reaction.

A value of 45.81 kJ/mol was determined for the activation energy E_a. This value should be compared with what is published in the literature by Bobeck and Su (1985), who reported 64.5 kJ/mol, and Mandre and

Sharma (1992), who reported 37.39 kJ/mol. For the second part of the reaction, where diffusion is needed for the leaching species to reach the surface of the sphalerite, an activation energy of 168.24 kJ/mol was determined. This large value indicates the magnitude of the energy barrier that needs to be overcome for the reaction to proceed.

7.7.2 Phase boundary controlled reaction

Habashi (1999) states that if a process is controlled by a chemical reaction at the interface (phase boundary controlled reaction), the equation $k_C t = 1-(1-R)^{1/3}$ applies. In figure 31 an attempt was made to demonstrate the relationship by plotting the fraction leached against time applying the different equations.

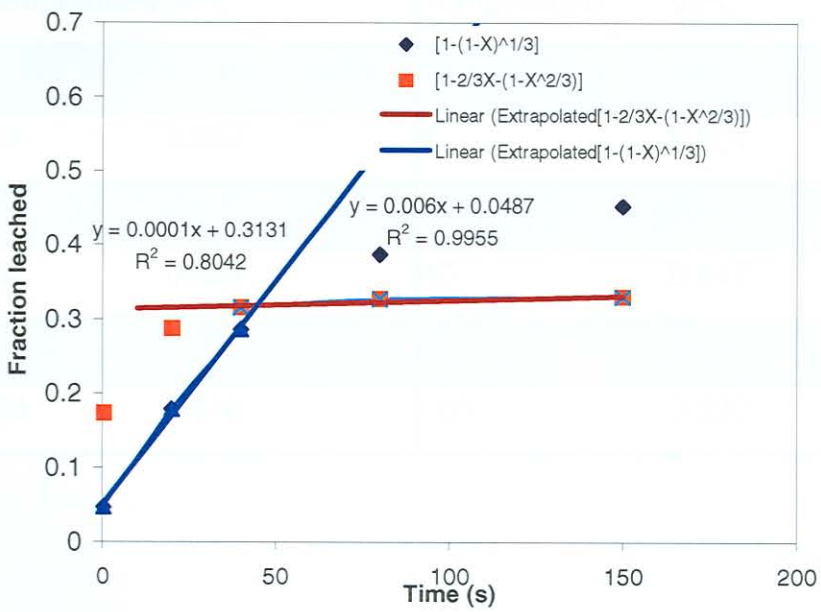

Figure 31: Plot of chemical and diffusion control models showing the conversion of ZnS to Zn^{2+} as a function of time according to equations 34 and 35 for establishing the rate-determining step. Leaching conditions 90° in 0.2 mol/dm^3 $FeCl_3$

From neither of the models a straight-line relationship could be deduced over the leaching range. At t < 45 minutes, it seems that the

process is controlled by the chemical reaction at the interface. At t > 45 minutes, it seems that the process is controlled by diffusion through the product layer. These results are similar to those reported by Lochman and Pedlik (1995).

7.7.3 Three-dimensional diffusion

In figure 32 an attempt was made to fit the three-dimensional diffusion model, as proposed by Jander (1927) (discussed in section 5.6.4). The results obtained from the test-work and represented in table 15 were applied to the model.

Table 15: Leach results

[$FeCl_3$]	0.2 mol/dm^3	[$FeCl_3$]	0.3 mol/dm^3
Temperature	90°C	Temperature	90°C
Time	Moles extracted	Time	Moles extracted
0.5	0.003	1	0.001
20	0.026	20	0.018
40	0.052	40	0.047
80	0.096	80	0.127
150	0.145	160	0.330

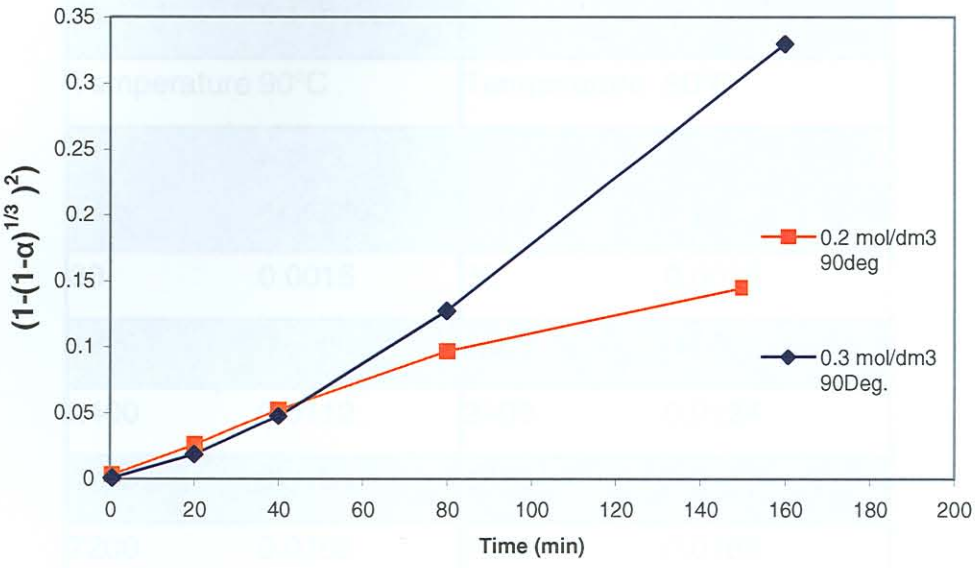

Figure 32: Plot of three-dimensional diffusion proposed by Jander (1927). Leaching conditions: 90°C in 0.2 and 0.3 mol/dm^3 $FeCl_3$ respectively

Reasonable curves were produced; the deviation from a straight line could be attributed to the shortcomings highlighted by Zeng and Heiningen (2002), (section 5.6.4). It will be noticed that up to about 40 minutes the two graphs are very much the same; after that point they seem to diverge. In figure 32, 40 minutes also seems to be the point where the two models diverge.

7.7.4 The mixed control model

The mixed control model (discussed in section 5.6.6) was applied to the data obtained in this study. Plots of the kinetic equations as functions of time, represented in figures 33 and 34, give almost perfectly straight lines.

The results obtained from the test-work and represented in table 16 were applied to the model.

Table 16: Leach results			
[$FeCl_3$]	0.1 mol/dm^3	[$FeCl_3$]	0.2 mol/dm^3
Temperature	90°C	Temperature	90°C
Time	Moles extracted	Time	Moles extracted
30	0.0015	30	0.0026
1200	0.0080	1200	0.0087
2400	0.0112	2400	0.0124
4800	0.0139	4800	0.0150
7200	0.0165	9000	0.0163

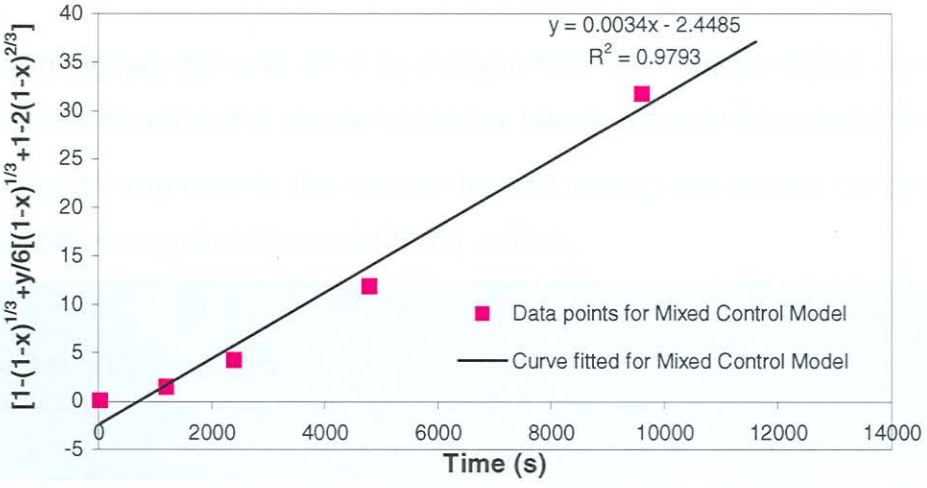

Figure 33: Plot of mixed control models showing the conversion of ZnS to Zn^{2+} as a function of time according to equation 60 (Huang and Rowson (2002)). Leaching conditions: 80°C in 0.2 mol/dm3 $FeCl_3$

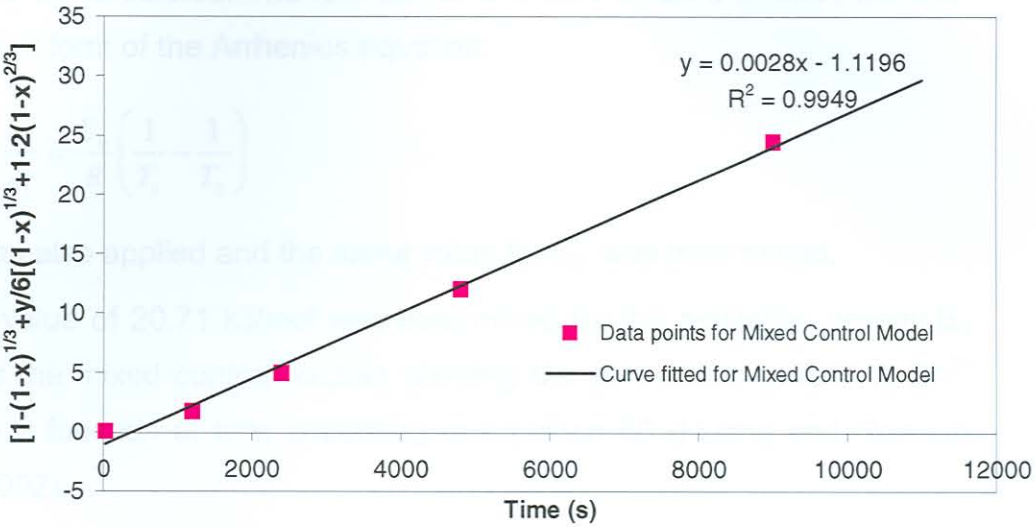

Figure 34: Plot of mixed control models showing the conversion of ZnS to Zn^{2+} as a function of time according to equation 60 (Huang and Rowson (2002)). Leaching conditions: 90°C in 0.2 mol/dm3 $FeCl_3$

From figures 33 and 34 it is evident that this kinetic model can be used to describe the reaction kinetics taking place in the reactions.

Table 17 represents the values for calculating the activation energy for the Huang and Rowson (2002) model.

Table 17: Calculations for the Arrhenius plot for the Huang and Rowson's (2002) model .

Starting sample	Temp (^{O}C)	Temp K	1/t (s^{-1})	k	Ln k
A 517 485	80	353	0.0028	0.0034	-5.683
A517-74	90	363	0.0027	0.0028	-5.878

The values ln k and 1/t in 17 table was plotted, the slope determined and E_a calculated. The formula for a limited amount of data, the two-point form of the Arrhenius equation:

$$\ln\frac{k_2}{k_1} = \frac{E_a}{R}\left(\frac{1}{T_1} - \frac{1}{T_2}\right)$$

was also applied and the same value for E_a was determined.

A value of 20.71 kJ/mol was determined for the activation energy E_a for the mixed control models showing the conversion of ZnS to Zn^{2+} as a function of time according to equation 60 (Huang and Rowson (2002).